Published in final edited form as:
Sci Transl Med. 2011 October 12; 3(104): 104ra101. doi:10.1126/scitranslmed.3002191.

DIABETES IMPAIRS HEMATOPOIETIC STEM CELL MOBILIZATION THROUGH ALTERATION OF NICHE FUNCTION

Francesca Ferraro[1,2,3,*], **Stefania Lymperi**[1,2,3,*], **Simón Méndez-Ferrer**[4], **Borja Saez**[1,2,3], **Joel A Spencer**[5,6], **Beow Y Yeap**[7], **Elena Masselli**[8], **Gallia Graiani**[10], **Lucia Prezioso**[10], **Elisa Lodi Rizzini**[8], **Marcellina Mangoni**[8], **Vittorio Rizzoli**[8], **Stephen M Sykes**[1,2,3], **Charles P. Lin**[5], **Paul S. Frenette**[9], **Federico Quaini**[10], and **David T. Scadden**[1,2,3]

[1]Center for Regenerative Medicine, Massachusetts General Hospital, Boston, Massachusetts 02114, USA

[2]Harvard Stem Cell Institute, Cambridge, Massachusetts 02138, USA

[3]Department of Stem Cell and Regenerative Biology, Harvard University, Cambridge, MA 02138, USA

[4]Cardiovascular Developmental Biology Department. Centro Nacional de Investigaciones Cardiovasculares, 28029 Madrid, Spain

[5]Advanced Microscopy Program, Center for System Biology and Wellman Center for Photomedicine, Massachusetts General Hospital, Boston, Massachusetts 02114, USA

[6]Department of Biomedical Engineering, Tufts University, Medford, Massachusetts 02155, USA

[7]Department of Medicine Massachusetts General Hospital, Boston, Massachusetts 02114, USA

[8]Department of Hematology and Bone Marrow Transplantation University of Parma, Parma, Italy

[9]Ruth L. and David S. Gottesman Institute for Stem Cell and Regenerative Medicine, Albert Einstein College of Medicine, Bronx, NY 10461, USA

[10]Department of Internal Medicine and Biomedical Science University of Parma, Parma 43100, Italy

Abstract

Autologous hematopoietic stem/progenitor cells (HSPC) transplantation success depends upon adequate cell collection after G-CSF-administration that a substantial fraction of patients fails to achieve. Retrospective analysis of patient records demonstrated that diabetes correlated with lower CD34+ cell mobilization. Using mouse models, we found impaired HSPC egress from the bone marrow in either streptozotocin-induced or *db/db* diabetic animals. HSPC aberrantly localized

Address for correspondence: David T. Scadden, 185 Cambridge St., Boston, MA 02114. dscadden@mgh.harvard.edu and Federico Quaini, Via Gramsci 14, 43100 Parma. federico.quaini@unipr.it.

*FF and SL contributed equally to the paper.

The paper describes a stem cell mobilization defect noted in clinical practice and defines both the basis for it and a pathophysiologically driven approach to overcome it using a mouse model.

Author contributions: FF and SL designed and performed experiments analyzed data and wrote the manuscript, SMF performed nerve quantitative analysis and RT-PCR on Nes+ cells and osteoblastic cells, analyzed data and edited the manuscript, BS performed experiments and edited manuscript, JSA helped with in vivo imaging experiments, BYY performed the statistical analysis on patient data, EM, GG, LP, ELR, MM, VR and PM performed the staining on human biopsies and analyzed human data, SMS performed experiments and edited the manuscript, CPL, PF contributed reagents and provided advice on the manuscript FQ and DTS supervised experiments and the overall study, and wrote the manuscript. All the authors have read the manuscript and agreed with his content.

Competing interest statement: DTS is a consultant to Fate Therapeutics, Genzyme, Hospira, Bone Therapeutics and a shareholder in Fate Therapeutics.

within the marrow microenvironment of diabetic animals in association with abnormalities in sympathetic neuron number and function. Markedly increased sympathetic neuron density was accompanied by abnormal response to β-adrenergic stimulation and a failure to generate the G-CSF-induced CXCL12 gradient in nestin-expressing mesenchymal cells associated with HSPC mobilization. Alternative mobilization by direct pharmacologic inhibition of CXCL12-CXCR4 interaction rescued the defect. These data reveal diabetes-induced changes in bone marrow physiology and microanatomy and point to a pathophysiologically based approach to overcome HSPC mobilization defects in diabetic patients.

Introduction

Hematopoietic stem and progenitor cell (HSPC) transplantation is a well-established therapy for benign and malignant blood diseases[1, 2]. Its clinical applications have steadily expanded to include certain solid tumors[3] and autoimmune disorders[4]. The success of HSPC transplantation highly depends upon a sufficient HSPC yield harvested from the blood. Granulocyte colony-stimulating factor (G-CSF), the mobilizing agent most widely used in clinics, elicits HSPC mobilization through several putative mechanisms[5]. These include proteolytic cleavage and downregulation of adhesion molecules and chemokines, the latter mediated at least in part by the sympathetic nervous system (SNS)[6, 7]. Among other effects, G-CSF increases sympathetic activity in the bone marrow microenvironment, where activation of β-adrenergic receptors in stromal cells inhibits CXCL12 synthesis[6, 7]. The resulting alteration in the CXCL12 gradient enables hematopoietic stem cells (HSCs) egress from the bone marrow[5, 8]. A significant fraction of transplant-eligible patients, referred to as ‘poor mobilizers’, do not achieve adequate levels of HSCs in the peripheral blood despite appropriate cytokine stimulation[9, 10]. With the exception of drug-induced myelotoxicity, it is largely unknown why these patients fail to mobilize. Reviewing a caseload of mobilization procedures performed over a 4-year period we observed elevated serum glucose levels and lower CD34+ cell concentrations in ‘mobilized’ blood in patients with diabetes. Using two distinct mouse models of diabetes we found that diabetes impairs HSC mobilization by altering perivascular neural and mesenchymal cell function and CXCL12 distribution in the bone marrow.

Results

High correlation of diabetes mellitus with patients who mobilize HSPC poorly

Autologous peripheral blood stem cell transplantation procedures performed in Parma Bone Marrow Transplantation Unit between 2004 and 2008 were reviewed (Supplementary table 1). We found an overall 22.6% (14/62) prevalence of mobilization failure, defined as <20 $CD34^+$ and <3000 polymorphonuclear (PMNs) cells/ml; <5,000 leukocytes/μl; <50,000 platelets/μl blood at the beginning of leukapheresis. The frequency of diabetes was 50% (7/14) in poor vs. 25% (12/48) in good mobilizers and was independent of age, gender and cycles of prior chemotherapy (Fig. 1A). Among the 48 patients that were able to appropriately mobilize, the amount of $CD34^+$ cells/kg was lower in diabetic compared to non-diabetic individuals (p=0.014, Fig. 1B). Additionally, glucose levels were significantly higher in poor mobilizers (p=0.002, Fig. 1C). There was a trend in slower neutrophil recovery (p=0.146) and significantly reduced platelet recovery (p=0.006) after peripheral blood stem cell transplantation of diabetic patients (p=0.146 and 0.006 respectively, Supplementary Fig. 1A and B). When poor mobilizers were transplanted with autologous bone marrow-derived cells the observed delayed engraftment of diabetic patients was more evident (p=0.002 and p=0.003, respectively; Supplementary Fig. 1C and D). All data are summarized in Supplementary Figure 1E.

HSPC Mobilization by G-CSF is impaired in animal models of diabetes

To investigate the mechanism underlying poor mobilization we evaluated HSPC mobilization in both a type I model of diabetes (induced by streptozotocin (STZ) treatment)[11] and a type II model of diabetes, the Leptin receptor knockout (*db/db*) mouse. In both settings, G-CSF injections (125 μg/kg every 12h for 4 days) were intraperitoneally (i.p.) administered to mobilize HSPCs. Flow cytometry of blood collected three hours after the last injection demonstrated significantly reduced percentages of Lin^- $Sca\text{-}1^+$ $c\text{-}Kit^+$ (LSK) cells in the circulation of STZ-treated mice (control, 0.072±0.016; diabetic, 0.024±0.008 n=5, p=0.03). Mobilized peripheral blood from these animals displayed a significant decrease in circulating colony-forming units in methylcellulose culture (CFU-C) (Fig. 1D) and diminished capacity to reconstitute hematopoiesis in lethally irradiated congenic recipients. Peripheral blood chimerism in recipient mice 4–16 weeks after transplantation was reduced by ~50% when mobilized blood was from diabetic compared to control animals (Fig. 1E). Similar results were observed when the same transplantation was performed using mobilized peripheral blood from *db/db* animals (Supplementary Fig. 2A). Since insulin deficiency characterizes type 1 (STZ-induced) and hyperinsulinemia type 2 (*db/db*) diabetes, we sought to determine whether the mobilization defect was associated with blood glucose concentration and/or insulin levels. The STZ-treated and *db/db* mice were stratified into four categories based on glucose levels. An inverse correlation between HSPC mobilization and blood glucose in both diabetes models was found, as measured by the number of circulating LSK and CFU-C (Fig. 1F–G and Supplementary Fig. 2B). Specifically, the Jonckheere-Terpstra test was used to assess the correlation between glucose levels and mobilization levels. An exact two-sided p-value was computed using StatXact 6.0 (Cytel Software Corp, Cambridge, MA). Higher blood glucose was associated with lower mobilization level in both STZ-treated (p=0.016) and *db/db* (p=0.006) mice. Plasma insulin concentration varied depending on the mouse model and was either low/absent (0.1± 0.2 ng/ml) or high (30±8 ng/ml) in the poorest mobilizer groups. It was within the normal range (1.1±0.3 ng/ml) in the groups with lower glycemic levels in either model. These results suggest that the rate of reduction in HSPC mobilization caused by diabetes is proportional to glucose unbalance and independent of insulin concentration.

Bone marrow HSC numbers are not affected in STZ-treated mice

Given the correspondence of the data between the model systems, only STZ-treated mice were the subjects of more detailed analyses. We assayed whether the reduction in circulating HSPC in diabetic mice was due to a reduced HSC content in steady state bone marrow. Percents and absolute numbers of LSK progenitor cells were increased in the bone marrow of diabetic mice (Fig. 2A), while total bone marrow cellularity was comparable to controls. This was in keeping with higher CFU-C formation per unit volume from diabetic bone marrow-derived cells (Fig. 2B). Long term-hematopoietic stem cells (LT-HSC) ($Lin^-Sca^+cKit^+CD150^+CD48^-$ and $Lin^-Sca^+cKit^+Flk2^-CD34^-$) percentage and absolute numbers were also increased in STZ-treated mice (Fig. 2C–D), this was accompanied by higher amount of proliferating HSPC and LT-HSC (Fig. 2E–F and Supplementary Fig 2C). In competitive repopulation assays the diabetic-derived bone marrow cells exhibited an advantage in long-term engraftment when injected into irradiated non-diabetic recipients (Fig. 2G–H). The correspondence between number of stem cells by flow cytometry and the repopulating ability in competitive transplantation suggests that LT-HSC have an intact repopulating potential per stem cell. Together, these results indicate that diabetic mice have an increased number of progenitor cells and LT-HSCs within the bone marrow despite exhibiting impaired HSC mobilization following G-CSF administration.

Increased adhesion and decreased chemotaxis of diabetic HSPC

To determine whether the defect in HSPC mobilization in diabetic mice was due to changes in their chemotactic or adhesive properties, purified LSK were subjected to *in vitro* migration and cell attachment assays. LSK isolated from STZ-treated mice demonstrated impaired migration to a CXCL12 gradient and increased adhesion to fibronectin *ex vivo* (Fig. 2I–J). The expression of surface antigens involved in HSPC retention and migration (CXCR4, L-selectin or CD62L, α4 integrin or CD49d, α5 integrin or CD49e) was analyzed by flow cytometry. CXCR4 expression on control LSK bone marrow cells was low with variable and non-significant increases in the setting of diabetes. $Alpha_4$ and $alpha_5$ integrin expression was unchanged while a significant increase in L-selectin levels was noted on diabetic LSK (Fig. 2K). To assess whether there might be increased activity of CXCR4 in response to CXCL12, we evaluated the calcium flux of diabetic and control LSK cells after CXCL12 exposure. No difference in calcium flux was observed between the two groups, suggesting that the disease did not affect CXCR4 down stream signaling. Overall, changes in HSPC migratory and adhesive activities were documented that could contribute to the observed phenotype.

Alterations in HSPC numbers and mobilization revert to normal when transplanted into a non-diabetic host

To determine whether the observed changes in HSPC migration, adhesion and antigen expression profile in STZ-treated mice persisted in a normal host, mice transplanted 16 weeks earlier with CD45.2 bone marrow cells from STZ- or saline-treated mice were treated with G-CSF (Fig. 3A). However, no difference in CFU-C mobilized into the blood was observed (Fig. 3B). Also, transplantation of irradiated animals with mobilized blood revealed that the contribution of the chimeric fractions (CD45.1/CD45.2 ratio) was equivalent in the two groups (Fig. 3C–D). These data indicate that cell autonomous alterations in function were not persistent and reverted in a non-diabetic host suggesting a primary role for the bone marrow (BM) microenvironment in the diabetes-related mobilization defect. Further, they exclude a direct, durable effect of STZ on HSPC accounting for their mobilization abnormality.

To assess whether the BM microenvironment was sufficient to induce the alterations in HSPC numbers and G-CSF response observed in diabetic mice, we transplanted equivalent numbers of wild-type CD45.1 bone marrow cells into lethally irradiated diabetic and control mice (Fig. 3E). 16 weeks post engraftment, bone marrow LSK were increased (Fig. 3F) with a trend to increased LT-HSC in diabetic recipients (Fig. 3G–H). When G-CSF was administered to these animals, the number of circulating CFU-C was lower in diabetic mice transplanted with WT cells (Fig. 3I). These results indicate that HSPC exposure to STZ was not required for the abnormalities in their function. Rather, persistent extrinsic signals from the abnormal, diabetic microenvironment or a rapidly reversible change in HSPC function are responsible for maintaining the mobilization defect associated with diabetes.

Diabetes alters bone marrow niche-cells

Following transplantation into irradiated recipients, LT-HSCs can be visualized in close proximity to the endosteal surface often positioned near osteoblastic cells and sinusoidal vessels [12–14]. They are retained in the BM by interactions with molecules such as kit ligand or stem cell factor (SCF) present on osteoblastic cells [15–19] and CXCL12 on a variety of cell types. Modulating CXCL12 levels are thought to be a requisite aspect of HSC mobilization from the BM into the blood[20–22].

Consequently, we examined microanatomic relationships, kit ligand and CXCL12 levels in the bone marrow in the setting of diabetes. Mice carrying a transgene in which GFP is

driven under the osteoblast-specific *Col2.3kb* promoter[23] or the *Nestin* promoter[24] (labeling mesenchymal stem cells) were used to identify cells composing the microenvironment.

a) Diabetes alters LT-HSC function in the bone marrow microenvironment— High-resolution confocal microscopy and two-photon video imaging was performed after injection of LT-HSCs in *Nes-Gfp* and *Col2.3-Gfp* transgenic mice. Briefly, calvarial BM was visualized following the injection of 5,000 dye-labeled LT-HSCs. The total number of HSCs and measurements of their distance relative to osteoblastic cells, the endosteal surface and Nes-GFP$^+$ cells were quantified in diabetic and control mice. Higher numbers of LT-HSCs were observed 24hrs after injection in diabetic mice compared to their controls (Fig. 4A). Clusters of 2, 3 or more DiD labeled cells were also observed at higher proportion in diabetic mice (Fig. 4B). To assess whether these events could be attributed to an increased chemoattractive ability of the diabetic marrow causing cell accumulation or to HSC proliferation, we injected a 1:1 mixture of FACS sorted LT-HSCs stained with the lipophilic cyanine dyes DiD or DiI. We found that cells in clusters were exclusively stained with one dye, consistent with migration and proliferation of a single cell, rather than co-localization of multiple injected HSCs (Fig. 4C). Further evaluation was conducted *in vitro* using DsRed-stained LSK CD48$^-$ cells cultured over a layer of stromal cells derived from control or diabetic mice. Despite several days of normoglycemic culture conditions (5.5 mM), diabetic stroma still promoted a 20% increase in HSPC growth compared to normal stroma ($p<0.01$, Supplementary Fig. 2D). Together with the higher fraction of cycling bone marrow cells found in diabetic mice ($p=0.05$, Supplementary Fig. 2E) and increased cell number detected by FACS and two photon video imaging, these data indicate that the diabetic stroma fosters HSPC proliferation.

The number of osteoblastic cells was significantly reduced in diabetic mice ($p<0.05$), while the number of Nes-GFP$^+$ cells did not change (Supplementary Fig. 2F–G). The latter result was also observed in human bone marrow biopsies, where the fraction of nestin$^+$ cells was similar in diabetic and non-diabetic patients (Supplementary Fig. 3A–D).

In addition, LT-HSCs were found in closer proximity to osteoblastic cells and to the endosteal surface in diabetic mice 24–48 hrs after transplantation (Fig. 4D). No difference was noted in location relative to nestin expressing perivascular cells. Assessment of mRNA levels of niche-related genes (CXCL12, V-cam1, SCF and angiopoietin-1) in osteoblastic cells revealed that, under steady state, the expression of SCF, previously associated with HSC lodgment in the endosteal region[17], was ~2-fold higher in diabetic mice (Fig. 4E), consistent with the observed closer proximity of HSCs. These data suggest that the diabetic microenvironment alters the lodgment and proliferation of normal HSCs.

b) Diabetes alters CXCL12 distribution within the bone marrow—Previous studies have shown that G-CSF-induced HSPC mobilization requires down-regulation of CXCL12 in the BM[25–27]. In steady state, Nes-GFP$^+$ cells are reportedly the major source of CXCL12 in mouse bone marrow[28]. In control mice, *Cxcl12* mRNA levels were >10-fold higher in Nes-GFP$^+$cells compared to osteoblastic cells (Fig. 4F). *Cxcl12* mRNA levels in Nes-GFP$^+$ cells were reduced by ~2-fold in diabetic animals compared with controls (Fig. 5A). Exposure to G-CSF had minimal impact on *Cxcl12* mRNA levels in Nes-GFP+ cells in the setting of diabetes while *Cxcl12* mRNA levels were efficiently down regulated in control mice (Fig. 5A). Thus, the magnitude of *Cxcl12* mRNA change following G-CSF administration was dramatically lower in diabetic animals compared to controls (92% versus 38%). This was the consequence of both lower baseline *Cxcl12* levels and failure of G-CSF to induce *Cxcl12* mRNA down-regulation. The lower mRNA level in diabetic mice was accompanied by a decrease in CXCL12 protein in Nes-GFP+ cells by flow cytometry (Fig.

5B). Despite these changes in cell type-specific mRNA levels, CXCL12 protein content in bone marrow extracellular fluids did not change (Fig. 5C) and peripheral blood actually had higher CXCL12 protein levels in diabetic mice ($p<0.05$, Supplementary Fig. 2I). Together, these results suggest that CXCL12 expression dynamics are changed in the diabetic microenvironment in a cell specific manner.

c. Cell depletion defines the role of osteoblasts in mobilization—To clarify the relative role of osteoblastic cells in the mobilization defect in diabetic settings, we employed the diptheria toxin (DT) system to selectively ablate these cells from STZ-treated and controls mice. Briefly, mice in which expression of Cre-recombinase was driven by the osteoblast specific Osteocalcin promoter[29] were crossed with mice harboring an inducible Diptheria Toxin Receptor transgene (iDTR) [30]. In the double transgenic, Cre-mediated removal of a transcriptional STOP cassette allows the expression of DT receptor. Upon DT administration, efficient ablation of the target population was achieved. Mice with only one transgene were used as controls. Diabetes was induced in both double transgenic (Oc-CRE-iDTR) and controls (Oc-CRE or iDTR). After deletion mice were treated with G-CSF or saline. Mobilized peripheral blood was transplanted in lethally irradiated congenic recipients along with support cells (Fig. 5D). Peripheral blood chimerism analysis at 4 weeks was used to define progenitor mobilization.

The data in Figure 5E reveal several issues. First, loss of osteoblasts increased the number of progenitors in the blood even without G-CSF. These data suggest that osteoblasts play a role in HSPC retention in the bone marrow. Second, with osteoblast depletion, G-CSF mobilization was compromised. Therefore, osteoblasts participate in the mobilizing ability of G-CSF; these two findings were in non-diabetic animals. In the presence of diabetes, a third point is raised, the depletion of osteoblasts completely abolished any residual mobilizing potential of G-CSF. These data suggest then that decreased osteoblasts observed in the bone marrow of diabetic animals may in part account for the poor retention and mobilization of HSPC. However, other cells must participate or the defect with osteoblast depletion without diabetes would have the same degree of compromise as the setting of osteoblast depletion and diabetes. Therefore, non-osteoblasts are a part of the STZ-induced mobilization defects.

Given that the mobilization process is proportional to the magnitude of the change of CXCL-12 levels in the BM microenvironment, it is reasonable to conclude that the nestin+ cells are likely non-osteoblast participant in G-CSF mediated progenitor cell release. This raises the issue of how nestin+ cell function is compromised by diabetes.

Increased sympathetic innervation and impaired response to β-adrenergic stimulation in diabetic bone marrow

To further assess potential mechanisms for compromised mobilization in diabetic animals, we evaluated sympathetic nervous system (SNS) cells that had been previously shown to participate in G-CSF-induced HSPC mobilization. Specifically, treatment with G-CSF was noted in prior studies to increase sympathetic activity in the BM, leading to *Cxcl12* mRNA downregulation in perivascular nestin$^+$ mesenchymal stem cells and HSPC release[6, 7]. We performed immunostaining for tyrosine hydroxylase, the rate-limiting enzyme in catecholamine synthesis, in the skull of diabetic and control mice. Catecholaminergic nerve terminals were increased by >2-fold in the calvarial bone marrow of diabetic mice (Fig. 6A–B). To determine whether increased catecholaminergic innervation was associated with altered sensitization of β-adrenergic receptors in Nes-GFP$^+$ cells, we treated diabetic and control *Nes-Gfp* transgenic mice with the β-adrenergic receptor agonist isoproterenol and measured *Cxcl12* mRNA levels two hours later (Fig. 6C–D). Reduced *Cxcl12* mRNA levels

in diabetic Nes-GFP$^+$ cells were confirmed under steady state. Further, the decrease in *Cxcl12* mRNA levels after isoproterenol treatment in control animals was markedly blunted in diabetic mice (Fig. 6C). Similar results were obtained from unsorted bone and trabecular bone marrow cells (Fig. 6D).

Activation of the β-adrenergic receptor is known to induce c-AMP-dependent protein kinase A (PKA) phosphorylation of the Threonine 197 residue in the catalytic subunit of PKA. Therefore, we assessed the level of phospho-PKA in sorted Nes-GFP$^+$ cells from control and diabetic mice both under baseline conditions and following isoproterenol administration (Fig. 6E). Isoproterenol markedly increased (~2.5 fold) the level of active PKA in control mice by Western blot using anti-phospho-T197-PKAα/β. Conversely, in diabetic mice showing higher baseline levels of phospho-PKA, isoproterenol induced only minor changes. β-adrenergic signaling in Nes-GFP$^+$ cells is mediated by binding to and activation of β3 adrenoreceptor, selectively expressed on nestin cells and absent on osteoblastic cells[28]. Therefore, we administered a selective β3 adrenergic blocker (SR59230A, Sigma) to diabetic mice and compared CXCL12 level to that of saline injected diabetic mice. CXCL12 levels in sorted Nes-GFP$^+$ cells were restored by β3 adrenergic blockade supporting the model of sympathetic hyperactivity causing aberrant CXCL12 regulation (Fig. 6F). These results are consistent with diabetes related sympathetic nervous system dysfunction perturbing the molecular axis governing HSPC mobilization by G-CSF.

SNS-independent HSPC mobilization is preserved in diabetes

The impairment in stem cell mobilization in diabetic mice was observed upon G-CSF challenging. G-CSF action relies at least in part on the functional integrity of SNS terminals, and because we could not find any phenotypical or functional alteration of CXCR4 in HSCs, we tested an alternative approach of HSPC mobilization that directly interferes with the interaction of CXCL12 with its cognate receptor, CXCR4. AMD3100 is a clinically used bicyclam antagonist that reversibly blocks the interaction between CXCL12 and CXCR4[31–34], prompting rapid HSPC mobilization. Mice were injected with 5 mg/kg AMD3100 and equal volumes of blood were transplanted in lethally irradiated non-diabetic recipients, together with supporting cells. Evaluation of chimerism at 4 weeks showed virtually complete mitigation of the diabetic mobilization defect as no significant differences in engraftment between mobilized diabetic and control HSPC were observed (Fig. 6G–H). AMD3100 alone is known to be a weak mobilizer compared to G-CSF[35, 36]. Concomitant administration of G-CSF and AMD3100 resulted in higher levels of donor chimerism and again demonstrated a rescue of the mobilization abnormalities previously noted in diabetic mice. These data are consistent with CXCL12 modulation in cells of the marrow microenvironment being the primary basis for the diabetes-induced mobilization defect.

Discussion

Our results demonstrate that STZ-treated mice closely mimic the impaired G-CSF induced mobilization observed in humans and that this defect is not the consequence of reduced bone marrow HSPC content or an intrinsic HSPC defect. Rather, the data support a model in which cells of the microenvironment are perturbed in diabetes and lose their ability to modulate CXCL12 in response to specific stimuli. The altered changes in CXCL12 expression may blunt HSPC release from the marrow and can be overcome by direct pharmacologic inhibitors of CXCL12-CXCR4 interaction.

The preservation or increase in HSPC number we observed is in contrast to recent reports of reduced LSK cells in diabetic mice[37, 38]. These differences may reflect species differences or may rely on the long term consequences of diabetes disease not assessed with this study. All mice used in our experiments were <12 weeks of age. For the STZ model, animals were

analyzed 5 to 8 weeks post induction. Furthermore, we performed both immunophenotypic and functional assays. It should be pointed out that discrepancies in the quantitative estimation of progenitor cells in diabetes has been observed in other tissues suggesting that the function rather than the quantity of progenitor cells may better define the deleterious effects of the disease[39, 40].

We documented some hematopoietic cell autonomous changes in diabetes such as reduced migratory ability and increased adherence to extracellular matrix components. Similar findings have been reported for other cell types in diabetic settings[41–44]. These properties of diabetic HSPC might participate in the altered mobilization capacity, however they were not retained after transplantation into non-diabetic hosts suggesting that the phenotype may be rapidly reversible. We did not further explore these features, rather we focused on whether abnormalities in the microenvironment were present. It has been described that hyperglycemia induces persistent epigenetic changes in stromal (endothelial) cells[45]. Correspondingly, we found that HSPC proliferation induced by diabetic bone marrow stromal cells was maintained even when cultured in normal glucose media for several days. Moreover, we showed that diabetic microenvironment is sufficient per se to induce early proliferation of transplanted wild type LT-HSC and this phenomenon is accompanied by changes in their localization. LT-HSCs tend to localize closer to the osteoblastic cells and the endosteal surface in diabetes at early and, most prominently, later time points. Importantly, diabetes reduced the number of osteoblastic cells supporting the notion that bone formation is impaired in patients affected by the disease. By selectively depleting osteoblasts, we showed that they participate in the residual ability of diabetic animals to mobilize to G-CSF, but that other cell types also contribute. We hypothesize that those other cells are the nestin+ mesenchymal stem cells that we defined have a defect in CXCL12 response to G-CSF in diabetes. HSPC mobilization by G-CSF has been defined by others to involve altering CXCL12 levels, [6, 7, 46]. This has been reported to occur through G-CSF altering SNS activity leading indirectly to down-regulation of CXCL12 levels[6,7]. SNS nerve terminals in the bone marrow are mainly located along arterioles and innervate perivascular cells[47],[28]. Perivascular nestin$^+$ mesenchymal stem cells have been shown to be innervated by SNS fibers, serve as a major source of CXCL12 in the mouse bone marrow, and downregulate *Cxcl12* in response to G-CSF or adrenergic stimulation[28]. Even though the overall content of CXCL12 in the bone marrow parenchyma was unchanged in STZ-treated animals, CXCL12 mRNA and protein levels in steady-state diabetic mice were reduced in stromal nestin$^+$ cells. Furthermore, the profound suppression of CXCL12 synthesis that follows G-CSF administration disappeared in nestin$^+$ cells from diabetic mice, suggesting that the loss of the chemokine directional gradient may be responsible for the defect in mobilization observed in diabetic settings. We also observed increased SNS terminals in diabetic calvaria bone marrow, associated with blunted response of nestin$^+$ cells to β-adrenergic agonists. It is known that diabetes is associated with increased sympathetic neural drive in humans[48, 49]. These results strongly suggest that diabetes-related dysautonomia may be responsible for impaired function of nestin$^+$ cells, leading to defective HSPC mobilization. However, given that G-CSF acts through multiple pathways to elicit HSPC mobilization[46], we cannot exclude the participation of additional mechanisms in the mobilization defect.

The importance of finding efficient mobilization strategies for diabetic patients is particularly evident in the light of the delayed engraftment observed when bone marrow-derived stem cells are used as a source for autologous transplantation. Normal HSPC mobilization in diabetic mice using AMD3100, which directly blocks CXCR4-CXCL12 binding, demonstrates that the disease does not affect this specific interaction providing a pathophysiologic rationale for the use of AMD3100 in the mobilization of HSPC for patients with diabetes. Finally, we found that nestin$^+$ cells with similar morphology and distribution

to the murine ones are also present in the human bone marrow, suggesting a possible similar role in human disease. Although the short-term diabetes model used may not reflect the late consequences of diabetes encountered in many patients, these studies serve as a guide for a more extensive evaluation of diabetic patients and provide a strong rationale for the use of alternatives to G-CSF for stem cell mobilization in patients with diabetes.

Material and methods

Diabetic mouse model

Diabetes was induced in 4–6 weeks old C57BL/6 (Jackson laboratory) *Nes-Gfp*[24] and *Col2.3-Gfp* (Jackson laboratory) male mice with five consecutive intraperitoneal injections of STZ dissolved in citrate buffer pH 4.5 (50 mg/kg/day). Mice were fastening for at least six hours before receiving the injection. Mice injected with citrate buffer alone were used as controls. B6.SJL-Ptprca Pep3b/BoyJ mice (SJL) (Jackson Laboratory) were employed as transplant recipients. Diabetes onset was confirmed by measuring insulin levels (Ultra Sensitive Mouse Insulin ELISA, Cristal Chem. INC.) and blood glucose (GlucoMeter One Touch Ultra TM). Only animals with glucose values higher than 300 mg/dl in a single measurement and concomitant low/absent level of insulin were further used for the experiments. Leptin receptor KO (db/db) mice were purchased from Jackson. All mice were housed according to IACUC guidelines and used for within 12–18 weeks of age.

Experimental HSC mobilization and blood collection

Recombinant human G-CSF (Neupogen, Filgrastrim) was administered at the dose of 125 μg/kg every 12 hours for 8 consecutive intraperitoneal injections. AMD3100 (Sigma) was employed at 50 mg/kg in single dose. PB samples were obtained through retro orbital bleeding three hours after the last injection of G-CSF and one hour after AMD3100 injection. In detail, mice were anesthetized using a mixture of Ketamine and Xylazine and blood was collected from the retro-orbital venous plexus through a microcapilary heparinized tube.

Flow cytometry and cell cycle analysis

Hematopoietic stem progenitors were identified based on their expression of lineage markers as well as c-Kit, Sca-1 and CD48, CD150 or CD34, CD135 (Flk-2) expression. Lineage staining was performed using a cocktail of biotinylated anti-mouse antibodies to Mac-1α (CD11b), Gr-1 (Ly-6G and Ly-6C), Ter119 (Ly-76), CD3, CD4, CD8a (Ly-2), and B220 (CD45R) (BD Biosciences). For detection we used lineage-streptavidin conjugated with PacOrange (Invitrogen), c-Kit-APC (CD117), CD48-FITC or PeCy5 (CD34), CD150-PE (CD135) and Sca1-APC-Cy7 or PeCy7 (BD Biosciences). For congenic strain discrimination, anti-CD45.1-APC and anti-CD45.2 FITC antibodies (BD Biosciences) were used. Adhesion molecules expression profile CXCR4, CD49D, CD49E, CD62L were all PE conjugated (e-Bioscience). CXCL12 labeling was performed using Monoclonal Anti-human/mouse CXCL12 Antibody Clone 79018 after fixation and permeabilization (BD cytofix/cytoperm kit) followed by secondary goat anti-mouse IgG-PE (both from R&D systems). For cell cycle staining cells were fixed overnight in 70% ethanol, washed twice in PBS and stained with a solution containing propidium iodide, RNAse A in Triton X 0.1%. For cell cycle staining in HSPC 18*10^6 BM cells were first stained with LSK and SLAMS markers then fixed and permeabilized (BD cytofix/cytoperm kit) and incubated with Ki-67 FITC (BD) 1:50 for 20 min at 4 degree. After washing, cells were resuspended in 600 uL washing buffer. 5 uL of a 1 mg/ml DAPI solution was added to cell suspension. Acquisition was conduced using LSRII (BD) after 30 minutes. Compensation and data analysis were performed with Flowjo 8.5.3.

CFU-C assay

Colony-forming unit assay (CFU-C) was performed as previously described [53]. Briefly, bone marrow derived cells or 50 uL of ACK-lysed PB cells were seeded into methylcellulose (StemCellTechnologies, M3434). Overall number of colonies was scored after 10 days.

Experimental PB transplantation

150 uL of blood from mobilized STZ-treated and control CD45.2 mice was mixed with 10^6 CD45.1 support cells and injected into lethally irradiated (9.5 Gy) SJL-45.1 recipients in the tail vein. Engraftment was monitored at four weeks intervals by enumerating donor CD45.1/.2$^+$ cells in the PB by FACS analysis.

Bone marrow cell isolation

Mice were sacrificed via CO_2 asphyxia; tibiae, femurs, and spine were removed and excess soft tissue was eliminated. Using a pestle and mortar, the bones were crushed and washed in PBS with 0.5% FBS and passed through a 40μm filter into a collection tube. Cells were spun at 1500rpm for 5 minutes; the supernatant was removed, and cells were then further processed for staining, sorting or for transplantation.

Collagenase treatment of bone

Bones were cracked in order to remove bone marrow content. Bone fragments were further cut into small fragments and transferred into a pre-warmed collagenase solution (StemCellTechnologies). Digestion was preformed for 1 hr at 37 °C under vigorous shaking. The solution was then filtered through a 40μm filter. The flow-through was then pelleted and further processed for FACS sorting or RNA extraction.

RNA isolation and quantitative real time RT-PCR

Nestin and Col2.3 cells were FACS sorted for GFP protein directly into lysis buffer and RNA isolation was performed using the Dynabeads mRNA DIRECT ™ Micro kit (Invitrogen). Primer sequences and RT-PCR procedure used have been previously described[28].

Experimental bone marrow transplantation

All bone marrow transplantations were performed by tail vein injection. For competitive transplantation, 10^6 whole bone-marrow cells from diabetic or control (CD45.2) mice were mixed with 10^6 CD45.1$^+$ (competitor) wild type cells and injected into lethally irradiated (9.5 Gy, one dose on the day of transplant) recipient BL6-SJL (CD45.1+) mice. Engraftment efficiency in recipients was monitored by donor contribution of CD45.2$^+$ cells using FACS analysis.

Adhesion and migration assays

For adhesion assays—2×10^3 FACS sorted LSK cells were plated in triplicate on 24-well culture-dishes pre-coated with fibronectin. The adherent fraction was dissociated by treatment with Cell Dissociation Buffer, enzyme-free (Invitrogen), collected and plated in MethoCult media (M3434, Stem cell technologies). Progenitor adhesion was determined as the percentage of CFU-C in the adherent fractions, relative to the frequency of CFU-C in the input sample.

For migration assays—2×10^3 FACS sorted LSK cells were suspended in 500 uL of RPMI and seeded in triplicate in the upper chamber of 24-well, 5-um Transwell plates

(Corning, Lowell, MA). Cells were incubated for 1 h at 37°C in the absence or presence of SDF1-α, after which the supernatant was removed and the wells were washed once with PBS to remove non-adherent cells. Adherent cells were harvested by treatment with Cell Dissociation Buffer, enzyme-free (Invitrogen) and plated in methylcelullose. Progenitor adhesion was determined as above mentioned.

Imaging of the HSC niche

Mice were anesthetized and prepared for the in vivo imaging as previously described[54] FACS sorted HSC were stained in PBS for 15 minutes at 37°C with DiD (1,1′-dioctadecil-3,3,3′-tetramethylindodicarbocyanine perchlorate, Invitrogen) or DiI (1,1′-dilinoleyl-3,3,3′,3′-tetramethylindocarbocyanine perchlorate, Invitrogen) using a 1:200 dilution and injected into lethally irradiated recipients. An approximately 4×6 mm area of the calvarium comprising the central sinus and the surrounding bone marrow cavities within the left and right frontal bones was scanned. When using Col2.3GFP and nestinGFP reporter mice, 3D models of the osteoblastic or nestin cells and the bone (second harmonic generation) were developed through Z-stack reconstruction. Using the Pythagoric theorem the location of stained HSC injected in relation to the bone and the GFP^+ cells was determined. The images were analyzed using Image J software (available free of charge by NIH in the website http://rsbweb.nih.gov/ij/).

Immunostaining of mice calvaria

Calvaria from diabetic and control mice were fixed in 4% paraformaldehyde for 1 h and subsequently washed twice in PBS. Blocking of unspecific binding and permeabilization were achieved with 20% goat serum and 0.5% TritonX-100 in PBS overnight. Endogenous biotin was blocked using Vector Kit (Cat # Sp-2001) following manufacturer instructions. Primary antibody (Chemicon rabbit anti-tyrosine hydroxylase; BD Pharmingen APC-conjugated anti-CD31) was applied at 1:100 in 20% goat serum, 0.1% Triton in PBS and incubated for 2–3 days. Samples were washed with 0.1% Triton in PBS and incubated overnight with a secondary biotinylated goat anti-rabbit antibody (1:200) in 20% goat serum, 0.1% Triton in PBS. After washing with 0.1% Triton in PBS samples were incubated for 2 hrs with ABC kit (Vector PK-6100) prepared 30 min before use. Following washes with PBS samples were incubated with Cy3-Tyramide (PerkinElmer) 1:200 in diluent reagent for 30 min, washed with PBS and visualized under fluorescence microscopy. Projections of Z-stacks (100–200 microns) of calvaria bone marrow were analyzed using the SlideBook® software (Intelligent Imaging Innovations).

Drugs administration

A single injection of isoproterenol (Sigma; 5 mg/kg: i.p.) was administered to diabetic and control mice. SR 59230A (Sigma; 5 mg/kg: i.p) was administered daily for 10 days to diabetic mice.

Mice treated with saline were used as a control. Animals were sacrificed 2 hours after injection by CO_2 asphyxia and the femora were flushed with 200 uL of PBS. Trizol (Invitrogen) was used for total RNA extraction.

Osteoblastic cell deletion

Mice in which expression of Cre-recombinase was driven by Osteocalcin promoter[29] were crossed with mice harboring an inducible Difteria Toxin Receptor transgene (iDTR) [30]. In the double transgenic, Cre-mediated removal of a transcriptional STOP cassette allows the expression of DT receptor. Upon DT administration efficient ablation of the target population was achieved. Mice with only one transgene were used as controls. Both double

and single transgenic mice were treated with either STZ for diabetes induction or with saline. After 5 weeks, DT was administered at the dose of 100 ng per mouse twice a day for 14 days. Nine days after starting the toxin administration G-CSF was administered (8 injections of 125 ugr/kg every 12 hrs). At days 14, blood was collected and used for flow and transplantation assays.

ELISA

CXCL12 protein levels were assessed in bone marrow supernatant and PB plasma. Briefly femurs from diabetic and control mice were flushed 4 times using 100 uL of PBS (total volume) in Eppendorf tubes. PB was collected via retroorbital bleeding in Eppendorf tubes without adding anti-coagulant. The samples were then incubated at 37°C for 1 hr and spun at 4.6 rpm for 5 min. Plasma was then collected and used for CXCL12 evaluation with ELISA kit (Ray Biosystem) following manufacturer instructions. Insulin levels were assessed in PB plasma with ELISA kit (Crystal Chem. Inc) following manufacturer instructions.

Western blot

Nestin-GFP cells were sorted using FACS-aria. Western blot was performed using antibody antPhopho-PKA (Invitrogen) following manufacturer instruction.

Statistical analysis

Mice—Unless otherwise specified, unpaired, 2-tailed Student's t test was used and data have been plotted as average ± s.e.m. Statistical significance is indicated by * ($p<0.05$) or ** ($p<0.01$) or *** ($p<0.001$).

Human—Fisher's exact test was used to compare the frequency of diabetes between poor and good mobilizers. The Wilcoxon two-sample test was used to compare the distribution of $CD34^+$ cell/kg and glucose levels between patient groups. Neutrophil recovery and platelet engraftment were measured from the day of transplantation with peripheral blood stem cells or bone marrow harvested cells. The cumulative incidence of engraftment was estimated using the Kaplan-Meier method, and the difference between diabetic and non-diabetic patients was assessed by the logrank test. All p-values were based on a two-sided hypothesis and were computed using SAS 9.2. (SAS Inst.).

Supplementary Material

Refer to Web version on PubMed Central for supplementary material.

Acknowledgments

We thank David Dombkowski, Laura B. Prickett-Rice, Kat Folz-Donahue, Sutanuka Lahiri for cell sorting expertise. We are grateful for help and advice to Cristina Lo Celso.

Funding: FF was supported by fellowships from Collegio Ghislieri, Associazione Italiana Leucemie and Associazione Cristina Bassi. SMF is thankful to ASH for the supporting scholarship. PF was funded by NIH grants R01HL097819 and R01DK056638. FQ was supported by the following grants: FP7-BIOSCENT, NMP- 214539 2007; PRIN AL2YNC 2007; Italian Ministry of Health THEAPPL 2008.

References

1. Appelbaum FR. Hematopoietic-cell transplantation at 50. N Engl J Med. 2007; 357:1472–1475. [PubMed: 17928594]

2. Thomas ED, Buckner CD, Sanders JE, Papayannopoulou T, Borgna-Pignatti C, De Stefano P, Sullivan KM, Clift RA, Storb R. Marrow transplantation for thalassaemia. Lancet. 1982; 2:227–229. [PubMed: 6124668]
3. Rick O, Siegert W, Schwella N, Dubiel M, Krusch A, Beyer J. High-dose chemotherapy as salvage treatment for seminoma. Bone Marrow Transplant. 2002; 30:157–160. [PubMed: 12189533]
4. Van Wijmeersch B, Sprangers B, Dubois B, Waer M, Billiau AD. Autologous and allogeneic hematopoietic stem cell transplantation for Multiple Sclerosis: perspective on mechanisms of action. J Neuroimmunol. 2008; 197:89–98. [PubMed: 18541311]
5. Lapidot T, Petit I. Current understanding of stem cell mobilization: the roles of chemokines, proteolytic enzymes, adhesion molecules, cytokines, and stromal cells. Exp Hematol. 2002; 30:973–981. [PubMed: 12225788]
6. Katayama Y, Battista M, Kao WM, Hidalgo A, Peired AJ, Thomas SA, Frenette PS. Signals from the sympathetic nervous system regulate hematopoietic stem cell egress from bone marrow. Cell. 2006; 124:407–421. [PubMed: 16439213]
7. Mendez-Ferrer S, Lucas D, Battista M, Frenette PS. Haematopoietic stem cell release is regulated by circadian oscillations. Nature. 2008; 452:442–447. [PubMed: 18256599]
8. Dar A, Kollet O, Lapidot T. Mutual, reciprocal SDF-1/CXCR4 interactions between hematopoietic and bone marrow stromal cells regulate human stem cell migration and development in NOD/SCID chimeric mice. Exp Hematol. 2006; 34:967–975. [PubMed: 16863903]
9. Hosing C, Saliba RM, Ahlawat S, Korbling M, Kebriaei P, Alousi A, De Lima M, Okoroji JG, McMannis J, Qazilbash M, Anderlini P, Giralt S, Champlin RE, Khouri I, Popat U. Poor hematopoietic stem cell mobilizers: a single institution study of incidence and risk factors in patients with recurrent or relapsed lymphoma. Am J Hematol. 2009; 84:335–337. [PubMed: 19384931]
10. Pusic I, Jiang SY, Landua S, Uy GL, Rettig MP, Cashen AF, Westervelt P, Vij R, Abboud CN, Stockerl-Goldstein KE, Sempek DS, Smith AL, DiPersio JF. Impact of mobilization and remobilization strategies on achieving sufficient stem cell yields for autologous transplantation. Biol Blood Marrow Transplant. 2008; 14:1045–1056. [PubMed: 18721768]
11. Like AA, Rossini AA. Streptozotocin-induced pancreatic insulitis: new model of diabetes mellitus. Science. 1976; 193:415–417. [PubMed: 180605]
12. Arai F, Hirao A, Ohmura M, Sato H, Matsuoka S, Takubo K, Ito K, Koh GY, Suda T. Tie2/angiopoietin-1 signaling regulates hematopoietic stem cell quiescence in the bone marrow niche. Cell. 2004; 118:149–161. [PubMed: 15260986]
13. Kiel MJ, Yilmaz OH, Iwashita T, Terhorst C, Morrison SJ. SLAM family receptors distinguish hematopoietic stem and progenitor cells and reveal endothelial niches for stem cells. Cell. 2005; 121:1109–1121. [PubMed: 15989959]
14. Sugiyama T, Kohara H, Noda M, Nagasawa T. Maintenance of the hematopoietic stem cell pool by CXCL12-CXCR4 chemokine signaling in bone marrow stromal cell niches. Immunity. 2006; 25:977–988. [PubMed: 17174120]
15. Huang EJ, Nocka KH, Buck J, Besmer P. Differential expression and processing of two cell associated forms of the kit-ligand: KL-1 and KL-2. Mol Biol Cell. 1992; 3:349–362. [PubMed: 1378327]
16. Papayannopoulou T, Priestley GV, Nakamoto B. Anti-VLA4/VCAM-1-induced mobilization requires cooperative signaling through the kit/mkit ligand pathway. Blood. 1998; 91:2231–2239. [PubMed: 9516120]
17. Driessen RL, Johnston HM, Nilsson SK. Membrane-bound stem cell factor is a key regulator in the initial lodgment of stem cells within the endosteal marrow region. Exp Hematol. 2003; 31:1284–1291. [PubMed: 14662336]
18. Ogawa M, Matsuzaki Y, Nishikawa S, Hayashi S, Kunisada T, Sudo T, Kina T, Nakauchi H. Expression and function of c-kit in hemopoietic progenitor cells. J Exp Med. 1991; 174:63–71. [PubMed: 1711568]
19. Czechowicz A, Kraft D, Weissman IL, Bhattacharya D. Efficient transplantation via antibody-based clearance of hematopoietic stem cell niches. Science. 2007; 318:1296–1299. [PubMed: 18033883]

20. Peled A, Petit I, Kollet O, Magid M, Ponomaryov T, Byk T, Nagler A, Ben-Hur H, Many A, Shultz L, Lider O, Alon R, Zipori D, Lapidot T. Dependence of human stem cell engraftment and repopulation of NOD/SCID mice on CXCR4. Science. 1999; 283:845–848. [PubMed: 9933168]
21. Wright DE, Bowman EP, Wagers AJ, Butcher EC, Weissman IL. Hematopoietic stem cells are uniquely selective in their migratory response to chemokines. J Exp Med. 2002; 195:1145–1154. [PubMed: 11994419]
22. Imai K, Kobayashi M, Wang J, Shinobu N, Yoshida H, Hamada J, Shindo M, Higashino F, Tanaka J, Asaka M, Hosokawa M. Selective secretion of chemoattractants for haemopoietic progenitor cells by bone marrow endothelial cells: a possible role in homing of haemopoietic progenitor cells to bone marrow. Br J Haematol. 1999; 106:905–911. [PubMed: 10519991]
23. Kalajzic I, Kalajzic Z, Kaliterna M, Gronowicz G, Clark SH, Lichtler AC, Rowe D. Use of type I collagen green fluorescent protein transgenes to identify subpopulations of cells at different stages of the osteoblast lineage. J Bone Miner Res. 2002; 17:15–25. [PubMed: 11771662]
24. Mignone JL, Kukekov V, Chiang AS, Steindler D, Enikolopov G. Neural stem and progenitor cells in nestin-GFP transgenic mice. J Comp Neurol. 2004; 469:311–324. [PubMed: 14730584]
25. Thomas J, Liu F, Link DC. Mechanisms of mobilization of hematopoietic progenitors with granulocyte colony-stimulating factor. Curr Opin Hematol. 2002; 9:183–189. [PubMed: 11953662]
26. Levesque JP, Hendy J, Takamatsu Y, Williams B, Winkler IG, Simmons PJ. Mobilization by either cyclophosphamide or granulocyte colony-stimulating factor transforms the bone marrow into a highly proteolytic environment. Exp Hematol. 2002; 30:440–449. [PubMed: 12031650]
27. Petit I, Szyper-Kravitz M, Nagler A, Lahav M, Peled A, Habler L, Ponomaryov T, Taichman RS, Arenzana-Seisdedos F, Fujii N, Sandbank J, Zipori D, Lapidot T. G-CSF induces stem cell mobilization by decreasing bone marrow SDF-1 and up-regulating CXCR4. Nat Immunol. 2002; 3:687–694. [PubMed: 12068293]
28. Mendez-Ferrer S, Michurina T, Ferraro F, Mazloom A, MacArthur B, Lira SA, Scadden DT, Ma'ayan A, Enikolopov GN, Frenette PS. Stem cell pairs, mesenchymal and hematopoietic, form a unique niche in the bone marrow. Nature. 2010
29. Zhang M, Xuan S, Bouxsein ML, von Stechow D, Akeno N, Faugere MC, Malluche H, Zhao G, Rosen CJ, Efstratiadis A, Clemens TL. Osteoblast-specific knockout of the insulin-like growth factor (IGF) receptor gene reveals an essential role of IGF signaling in bone matrix mineralization. J Biol Chem. 2002; 277:44005–44012. [PubMed: 12215457]
30. Buch T, Heppner FL, Tertilt C, Heinen TJ, Kremer M, Wunderlich FT, Jung S, Waisman A. A Cre-inducible diphtheria toxin receptor mediates cell lineage ablation after toxin administration. Nat Methods. 2005; 2:419–426. [PubMed: 15908920]
31. Hatse S, Princen K, Bridger G, De Clercq E, Schols D. Chemokine receptor inhibition by AMD3100 is strictly confined to CXCR4. FEBS Lett. 2002; 527:255–262. [PubMed: 12220670]
32. Liles WC, Broxmeyer HE, Rodger E, Wood B, Hubel K, Cooper S, Hangoc G, Bridger GJ, Henson GW, Calandra G, Dale DC. Mobilization of hematopoietic progenitor cells in healthy volunteers by AMD3100, a CXCR4 antagonist. Blood. 2003; 102:2728–2730. [PubMed: 12855591]
33. Shen H, Cheng T, Olszak I, Garcia-Zepeda E, Lu Z, Herrmann S, Fallon R, Luster AD, Scadden DT. CXCR-4 desensitization is associated with tissue localization of hemopoietic progenitor cells. J Immunol. 2001; 166:5027–5033. [PubMed: 11290783]
34. Broxmeyer HE, Orschell CM, Clapp DW, Hangoc G, Cooper S, Plett PA, Liles WC, Li X, Graham-Evans B, Campbell TB, Calandra G, Bridger G, Dale DC, Srour EF. Rapid mobilization of murine and human hematopoietic stem and progenitor cells with AMD3100, a CXCR4 antagonist. J Exp Med. 2005; 201:1307–1318. [PubMed: 15837815]
35. DiPersio JF, Stadtmauer EA, Nademanee A, Micallef IN, Stiff PJ, Kaufman JL, Maziarz RT, Hosing C, Fruehauf S, Horwitz M, Cooper D, Bridger G, Calandra G. Plerixafor and G-CSF versus placebo and G-CSF to mobilize hematopoietic stem cells for autologous stem cell transplantation in patients with multiple myeloma. Blood. 2009; 113:5720–5726. [PubMed: 19363221]

36. Flomenberg N, Devine SM, Dipersio JF, Liesveld JL, McCarty JM, Rowley SD, Vesole DH, Badel K, Calandra G. The use of AMD3100 plus G-CSF for autologous hematopoietic progenitor cell mobilization is superior to G-CSF alone. Blood. 2005; 106:1867–1874. [PubMed: 15890685]
37. Oikawa A, Siragusa M, Quaini F, Mangialardi G, Katare RG, Caporali A, van Buul JD, van Alphen FP, Graiani G, Spinetti G, Kraenkel N, Prezioso L, Emanueli C, Madeddu P. Diabetes mellitus induces bone marrow microangiopathy. Arterioscler Thromb Vasc Biol. 30:498–508. [PubMed: 20042708]
38. Orlandi A, Chavakis E, Seeger F, Tjwa M, Zeiher AM, Dimmeler S. Long-term diabetes impairs repopulation of hematopoietic progenitor cells and dysregulates the cytokine expression in the bone marrow microenvironment in mice. Basic Res Cardiol.
39. Asicioglu E, Gogas Yavuz D, Koc M, Ozben B, Yazici D, Deyneli O, Akalin S. Circulating endothelial cells are elevated in patients with type 1 diabetes mellitus. Eur J Endocrinol. 162:711–717. [PubMed: 20061332]
40. Hill JM, Zalos G, Halcox JP, Schenke WH, Waclawiw MA, Quyyumi AA, Finkel T. Circulating endothelial progenitor cells, vascular function, and cardiovascular risk. N Engl J Med. 2003; 348:593–600. [PubMed: 12584367]
41. Lan CC, Liu IH, Fang AH, Wen CH, Wu CS. Hyperglycaemic conditions decrease cultured keratinocyte mobility: implications for impaired wound healing in patients with diabetes. Br J Dermatol. 2008; 159:1103–1115. [PubMed: 18717678]
42. Bhatwadekar AD, Glenn JV, Li G, Curtis TM, Gardiner TA, Stitt AW. Advanced glycation of fibronectin impairs vascular repair by endothelial progenitor cells: implications for vasodegeneration in diabetic retinopathy. Invest Ophthalmol Vis Sci. 2008; 49:1232–1241. [PubMed: 18326753]
43. Loughlin DT, Artlett CM. 3-Deoxyglucosone-collagen alters human dermal fibroblast migration and adhesion: implications for impaired wound healing in patients with diabetes. Wound Repair Regen. 2009; 17:739–749. [PubMed: 19769726]
44. Azcutia V, Abu-Taha M, Romacho T, Vazquez-Bella M, Matesanz N, Luscinskas FW, Rodriguez-Manas L, Sanz MJ, Sanchez-Ferrer CF, Peiro C. Inflammation determines the pro-adhesive properties of high extracellular d-glucose in human endothelial cells in vitro and rat microvessels in vivo. PLoS One. 5:e10091. [PubMed: 20386708]
45. El-Osta A, Brasacchio D, Yao D, Pocai A, Jones PL, Roeder RG, Cooper ME, Brownlee M. Transient high glucose causes persistent epigenetic changes and altered gene expression during subsequent normoglycemia. J Exp Med. 2008; 205:2409–2417. [PubMed: 18809715]
46. Papayannopoulou T. Current mechanistic scenarios in hematopoietic stem/progenitor cell mobilization. Blood. 2004; 103:1580–1585. [PubMed: 14604975]
47. Yamazaki K, Allen TD. Ultrastructural morphometric study of efferent nerve terminals on murine bone marrow stromal cells, and the recognition of a novel anatomical unit: the “neuro-reticular complex”. Am J Anat. 1990; 187:261–276. [PubMed: 2321559]
48. Rosengard-Barlund M, Bernardi L, Fagerudd J, Mantysaari M, Af Bjorkesten CG, Lindholm H, Forsblom C, Waden J, Groop PH. Early autonomic dysfunction in type 1 diabetes: a reversible disorder? Diabetologia. 2009; 52:1164–1172. [PubMed: 19340407]
49. Straznicky NE, Eikelis N, Lambert EA, Esler MD. Mediators of sympathetic activation in metabolic syndrome obesity. Curr Hypertens Rep. 2008; 10:440–447. [PubMed: 18959829]
50. Akhter J. The American Diabetes Association’s Clinical Practice Recommendations and the developing world. Diabetes Care. 1997; 20:1044–1045. [PubMed: 9167126]
51. Jerkeman M, Leppa S, Kvaloy S, Holte H. ICE (ifosfamide, carboplatin, etoposide) as second-line chemotherapy in relapsed or primary progressive aggressive lymphoma--the Nordic Lymphoma Group experience. Eur J Haematol. 2004; 73:179–182. [PubMed: 15287915]
52. Velasquez WS, Cabanillas F, Salvador P, McLaughlin P, Fridrik M, Tucker S, Jagannath S, Hagemeister FB, Redman JR, Swan F, et al. Effective salvage therapy for lymphoma with cisplatin in combination with high-dose Ara-C and dexamethasone (DHAP). Blood. 1988; 71:117–122. [PubMed: 3334893]

53. Glimm H, Eaves CJ. Direct evidence for multiple self-renewal divisions of human in vivo repopulating hematopoietic cells in short-term culture. Blood. 1999; 94:2161–2168. [PubMed: 10498585]

54. Lo Celso C, Fleming HE, Wu JW, Zhao CX, Miake-Lye S, Fujisaki J, Cote D, Rowe DW, Lin CP, Scadden DT. Live-animal tracking of individual haematopoietic stem/progenitor cells in their niche. Nature. 2009; 457:92–96. [PubMed: 19052546]

A

2004-2008: Bone Marrow Transplantation Unit-University of Parma

	Non-diabetic	Diabetic	Total
Good Mobilizers >20 CD34$^+$ cells/uL	36 (75%)	12 (25%)	**48**
Poor Mobilizers <20 CD34$^+$ cells/uL	7 (50%)	7 (50%)	**14**
Total	**43**	**19**	**62**

Mobilization regimen: chemotherapy + G -CSF

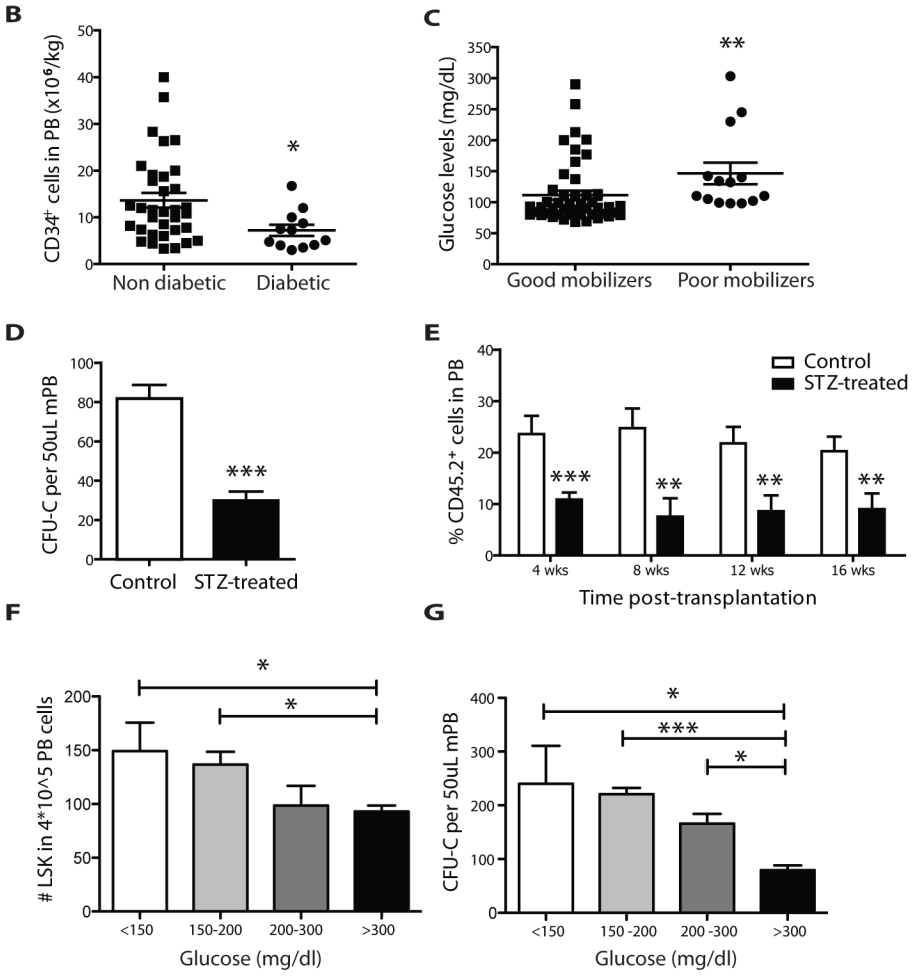

Figure 1. Diabetes reduces G-CSF-induced HSPC mobilization

(**A**) Table showing the actual numbers (and percentages) of patients mobilized with more than (good mobilizers) or less than (poor mobilizers) 20 CD34$^+$ cells/μL. Overall 22.6% (14/62) rate of mobilization failure. Frequency of diabetes is 50% (7/14) in poor vs. 25% (12/48) in good mobilizers (p=0.102) (**B**) Number of CD34$^+$ cells per kg in the PB of patients mobilized with 10 ug/kg/day G-CSF. Scatter plot showing mean ± s.e.m., n=36 non diabetic and n=12 diabetic. Diabetic patients mobilize CD34$^+$ cells more poorly (n=36 in non diabetic, n=12 diabetic * p<0.05), even among good mobilizers. (**C**) Glucose levels (mg/dl) in good mobilizers versus poor mobilizers. Scatter plot showing mean ± s.e.m. Higher glucose levels are found in poor mobilizers (n=14 poor mobilizers, n=48 good mobilizers **p<0.01). (**D**) Number of CFU-C per 50ul G-CSF-mobilized peripheral blood, obtained from STZ-treated or control mice. Columns represent mean ± s.e.m. n=12, *** p<0.001. (**E**) Percentages of total CD45.2$^+$ donor derived cells in the peripheral blood of lethally irradiated SJL recipients transplanted with 150 ul of G-CSF mobilized PB from

C57Bl/6 diabetic or control mice as assessed by FACS analysis at regular time intervals. Columns represent mean ± s.e.m., n=18, *** p<0.001, **p<0.01. (**F–G**) STZ-treated and controls mice were divided in four categories based upon peripheral blood glucose levels (<150, 150–200, 200/300 and >300 mg/dl). Histograms plots represent mean ± s.e.m. of (**F**) number of LSK in 4*10^5 total blood cells by flow cytometry, n=12, * p<0.05 and (**G**) number of CFU-C per 50ul of mobilized peripheral blood, n=12, * p<0.05, **p<0.01.

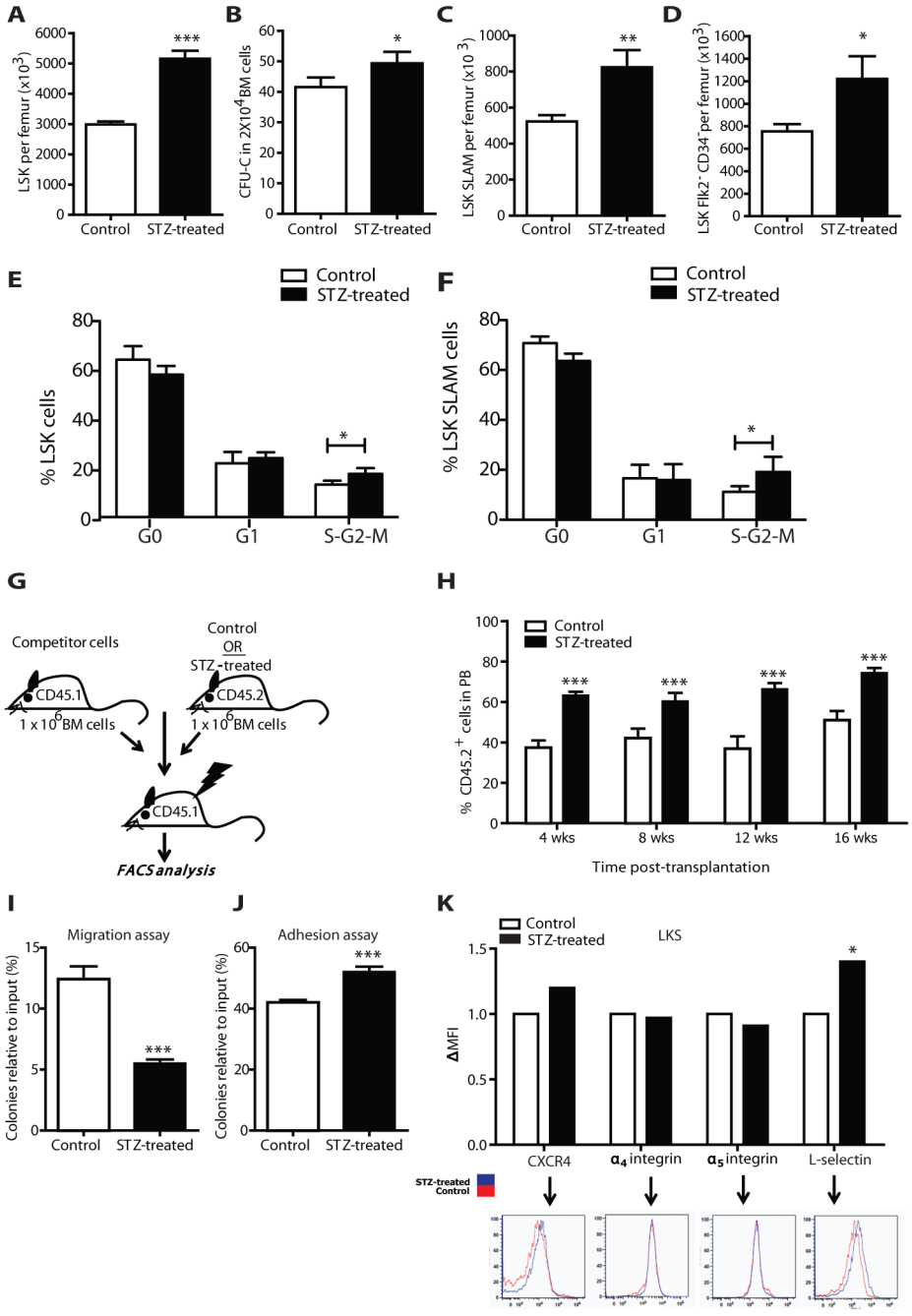

Figure 2. Characterization of the hematopoietic compartment in the BM of STZ-treated animals

(**A**) Number of LSK per femur defined by flow cytometry in STZ-treated or control mice. Data are mean ± s.e.m., n=24, *** p<0.001. (**B**) CFU-C numbers of BM cells obtained from STZ-treated and control mice. Data are mean ± s.e.m., n=6, * p<0.05. (**C**) Number of LT-HSC $Lin^{-}Sca^{+}cKit^{+}CD150^{+}CD48^{-}$ and (**D**) $Lin^{-}Sca^{+}cKit^{+}Flk2^{-}CD34^{-}$ per femur in STZ-treated or control mice as assessed by flow cytometry. Data are mean ± s.e.m., n=8, **p<0.01 and * p<0.05 respectively. (**E–F**) Histogram plots showing the fraction of LSK (**E**) and LT-HSC (**F**) in different phases of the cell cycle in STZ-treated versus control mice. Coloumns are mean ± s.e.m., n=4, * p<0.05. (**G**) Schematic representation of the transplantation experiment to assess the number/functionality of BM cells from STZ-

induced diabetic mice. (**H**) Donor-derived CD45.2$^+$ cell engraftment 4, 8, 12 and 16 weeks after transplantation in the peripheral blood of secondary SJL recipient mice transplanted with bone marrow isolated from STZ-treated or control mice and mixed with equal amount of CD45.1 competitor cells. Columns represent mean ± s.e.m., n=10, *** p<0.001. (**I**) CFU-C (relative to input) mean number ± s.e.m of the migrated purified LSK from STZ-treated or control mice toward CXCL12 (300ng/ml), n=6, *** p<0.001. (**J**) FACS-sorted LSK from control or STZ-treated mice were plated onto 24-well plates previously coated with 10μg/ml fibronectin. After 4 hours the adhesive LSK content was plated into methylcellulose. Data are mean CFU-C number relative to input ± s.e.m., n=6, *** p<0.001. (**K**) Representative FACS plots and bars indicating delta mean fluorescence intensity (DMFI) over controls showing the expression levels of CXCR4, α_4 integin, α_5 integin, and L-selectin in LSK isolated from STZ-treated and control mice, n=9, * p<0.05.

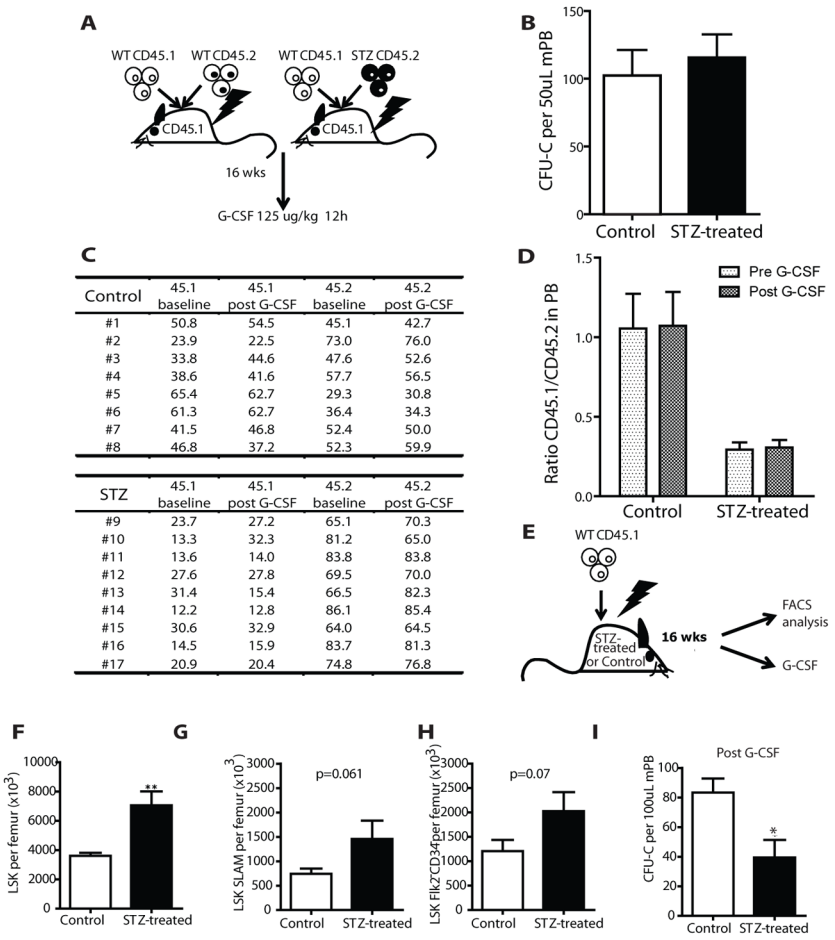

Control	45.1 baseline	45.1 post G-CSF	45.2 baseline	45.2 post G-CSF
#1	50.8	54.5	45.1	42.7
#2	23.9	22.5	73.0	76.0
#3	33.8	44.6	47.6	52.6
#4	38.6	41.6	57.7	56.5
#5	65.4	62.7	29.3	30.8
#6	61.3	62.7	36.4	34.3
#7	41.5	46.8	52.4	50.0
#8	46.8	37.2	52.3	59.9

STZ	45.1 baseline	45.1 post G-CSF	45.2 baseline	45.2 post G-CSF
#9	23.7	27.2	65.1	70.3
#10	13.3	32.3	81.2	65.0
#11	13.6	14.0	83.8	83.8
#12	27.6	27.8	69.5	70.0
#13	31.4	15.4	66.5	82.3
#14	12.2	12.8	86.1	85.4
#15	30.6	32.9	64.0	64.5
#16	14.5	15.9	83.7	81.3
#17	20.9	20.4	74.8	76.8

Figure 3. Altered mobilization ability in diabetic mice is not cell autonomous but microenviroment dependent

(**A**) Schematic representation of the procedure followed to assess whether the inhibition of mobilization is cell autonomous or microenvironment dependent. Lethally irradiated SJL recipients were transplanted with 1×10^6 BM cells from STZ-treated or control mice, along with 1×10^6 CD45.1 support cells. 16 weeks after transplantation the SJL recipients from the two groups underwent G-CSF mobilization regimen. (**B**) Number of CFU-C in the PB of recipients transplanted with STZ-treated or control cells after the induction of mobilization with G-CSF. Columns represent mean ± s.e.m., n=8. (**C**) Actual numbers and (**D**) ratio of CD45.1 and CD45.2 positive cells in the peripheral blood of recipient mice transplanted with STZ-treated or control cells before and after mobilization with G-CSF treatment. Columns represent mean ± s.e.m., n=9 and 8 respectively. (**E**) Schematic representation of the reverse experiment in which 15 STZ-treated and control C57Bl6 mice were transplanted with wild type CD45.1 whole bone marrow cells. After 16-weeks 10 mice were evaluated for LSK and LT-HSC numbers. 5 mice underwent G-CSF mobilization therapy followed by blood collection and evaluation of CFU-C number. (**F**) Graph bars represent number of LKS per femur. Data are mean ± s.e.m., n=10, ** $p<0.01$. (**G**) Number per femur of LT-HSC $Lin^-Sca^+cKit^+CD150^+CD48^-$ and (**H**) Lin- $Lin^-Sca^+cKit^+Flk2^-CD34^-$ as assessed by flow cytometry. Data are mean ± s.e.m., n=10. (**I**) Number of CFU-C per 100 μl of G-CSF-mobilized peripheral blood from STZ-treated and control mice 16 weeks after transplantation, data are mean ± s.e.m., n=5, * $p<0.05$.

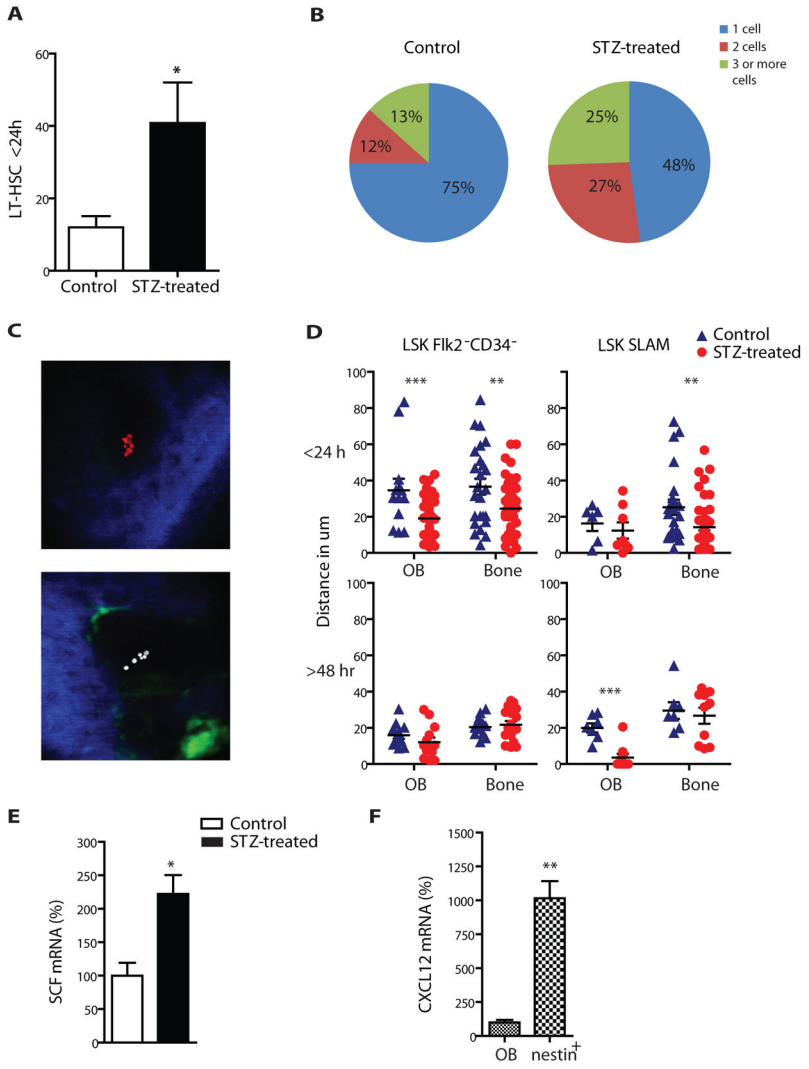

Figure 4. Altered LT-HSC function in the bone marrow microenvironment of diabetic mice

(**A**) Number of wild type LT-HSC found within 24 hours in the calvaria BM cavity of control or STZ-treated recipients with the in vivo imaging. n=8, * $p<0.05$. (**B**) Percentages of 1, 2 or 3 and more cell clusters found in the BM cavity of control and STZ-treated recipients. (**C**) Representative pictures of the BM cavity of STZ-treated mice injected with equal numbers of DiD and DiI labelled HSCs. Blue=second harmonic generation signal (bone), green=Col2.3GFP (osteoblastic cells), red=DiD labeled cells (LT-HSC), white=DiI labeled cells (LT-HSC). (**D**) Distances of $Lin^{-}Sca^{+}cKit^{+}Flk2^{-}CD34^{-}$ and $Lin^{-}Sca^{+}cKit^{+}CD150^{+}CD48^{-}$ cells 24 and 48 hours after transplantation relative to the Col2.3GFP cells and bone (measure in μm). (**E**) Percentage changes in SCF (*kitl*) mRNA levels in sorted $col2.3GFP^{+}$ osteoblastic cells between STZ-treated and control mice normalised to GAPDH (ΔΔCTmethod). Columns represent mean ± s.e.m.. n=6, * $p<0.05$ (**F**) Percentage difference in *Cxcl12* mRNA levels in steady state condition among nestin cells and osteoblastic cells. n=6, ** $p<0.01$

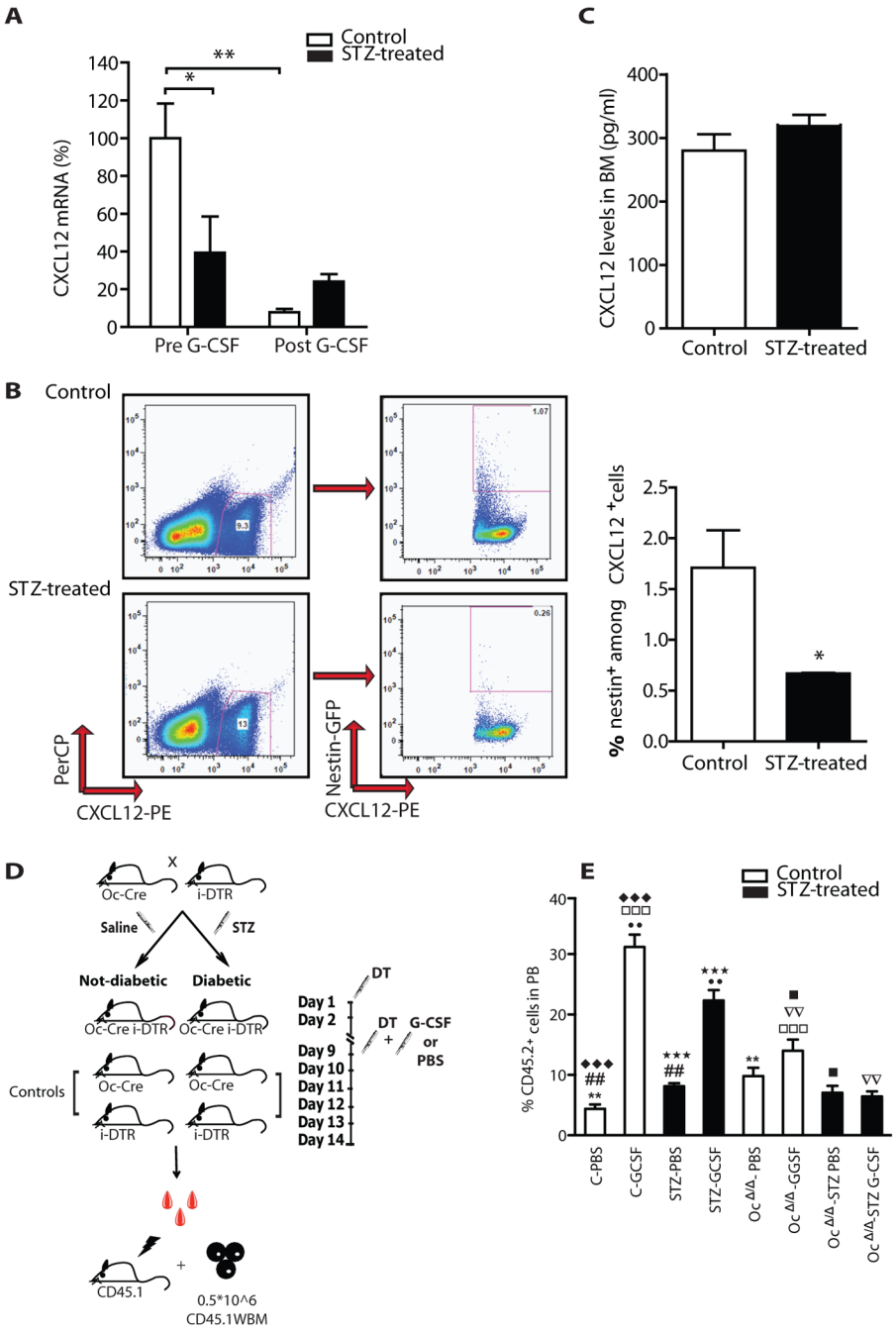

Figure 5. STZ-induced diabetic mice have aberrant expression of niche related molecules

(**A**) Percent changes in the expression of mRNA levels of *Cxcl12* in FACS sorted nestinGFP$^+$ cells before and after G-CSF treatment relative to control nestinGFP$^+$ cells before G-CSF treatment and normalised to GAPDH (ΔΔCTmethod). Columns represent mean ± s.e.m., n=6 * p<0.05 and **p<0.01. (**B**) Representative FACS plots and graph bars showing percentages of CXCL12$^+$ cells among nestin$^+$ cells. Data are mean ± s.e.m., n=6, * p<0.05. (**C**) Concentration (pg/ml) of CXCL12 in BM extracellular fluid from control and STZ-treated mice. Data are mean number ± s.e.m., n=6. (**D**) Schematic representation of the experimental design used to selectively disrupt osteoblastic cells (see methods). (**E**) Donor-

derived CD45.2^{+} cell engraftment 4 weeks after transplantation of mobilized peripheral blood in lethally irradiated SJL recipients. Columns represents mean± s.e.m., n=8 in each group, ◆◆◆, □□□, ★★★ p<0.001 **, ●●, ▽▽, ## p<0.01, ■ p< 0.05

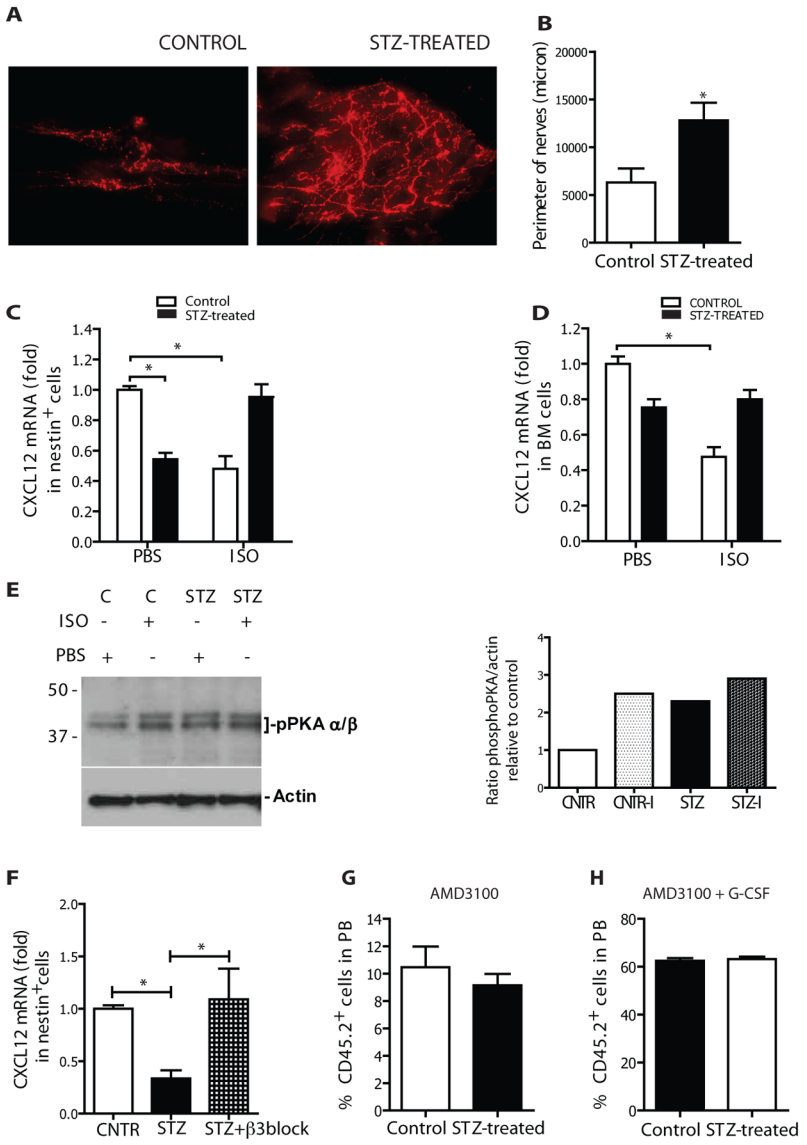

Figure 6. PNS disautonomy is responsible for deregulation of CXCL12 gradient

(**A**) Representative pictures from whole mounting of calvaria of controls (left picture) and STZ-treated mice (right picture). Red signal: tyrosine hydroxilase. Scale bar: 50 μm. Nerve terminal quantification in terms of perimeter (**B**) in calvaria of STZ-treated versus controls mice n=5 *p<0.05. Fold changes in the expression of mRNA levels of CXCL12 in (**C**) nestin+ cells (**D**) bone marrow from control and STZ-treated mice in baseline conditions and 2 hrs after injection of isoproterenol (5 mg/kg i.p) relative to control cells in baseline and normalised to GAPDH (ΔΔCTmethod). n=6, *p<0.5. (**E**) Left: Western blot showing the amount of phospho-PKA (pPKA) in sorted nestin+ cells from control (+/− isoproterenol) and STZ-treated (+/− isoproterenol) mice. Right: Histogram plot showing ratio in pPKA. (**F**) Fold changes in the expression of mRNA levels of *Cxcl12* in nestin+ cells from diabetic saline treated and diabetic β3 -blocker treated (5 mg/kg/day for 10 days) animals relative to non-diabetic controls. Data are normalized to GAPDH (ΔΔCTmethod). n=6, *p<0.5. Percentage of donor cell engraftment 4 weeks after transplantation of 150 μL of mobilized-PB from STZ-treated and control mice (along with whole bone marrow support cells) in

congenic lethally irradiated recipients. Mice were mobilized with single dose of AMD3100 (**G**) or single dose of AMD3100 at the end of the G-CSF mobilization regimen (**H**), n=5.